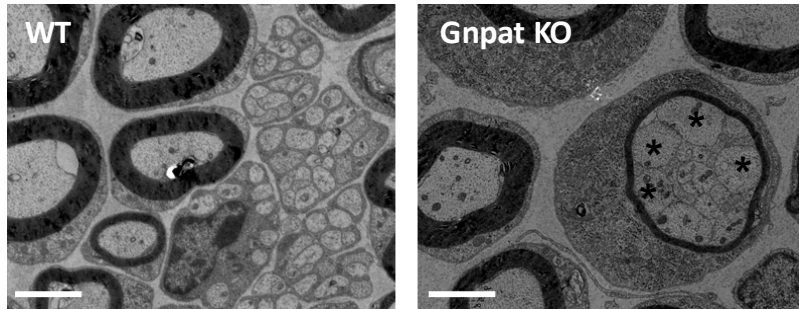
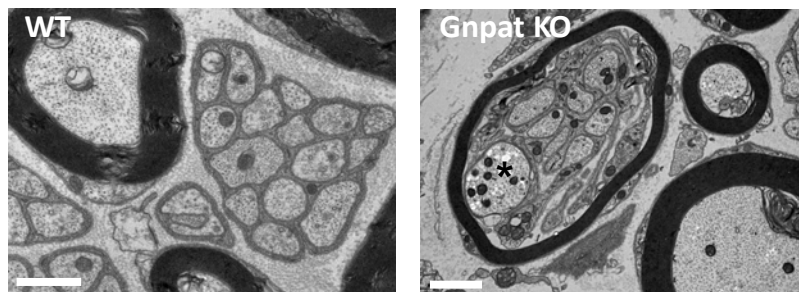


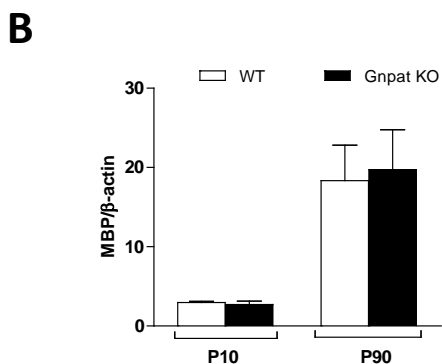
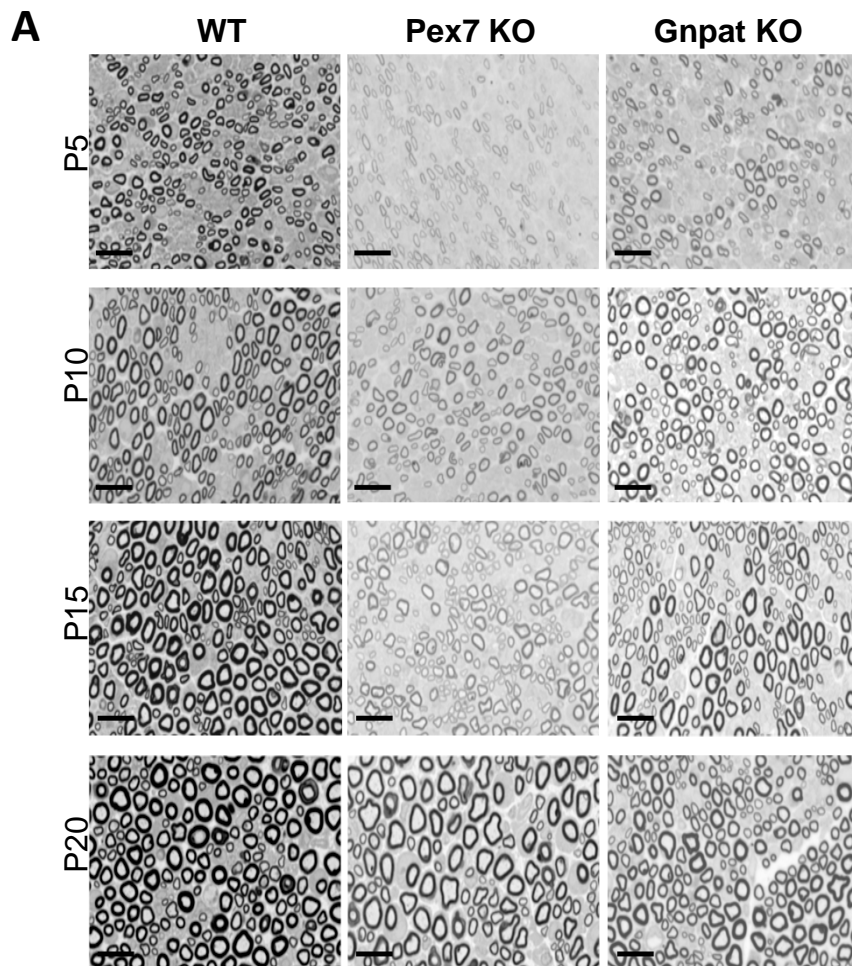
A



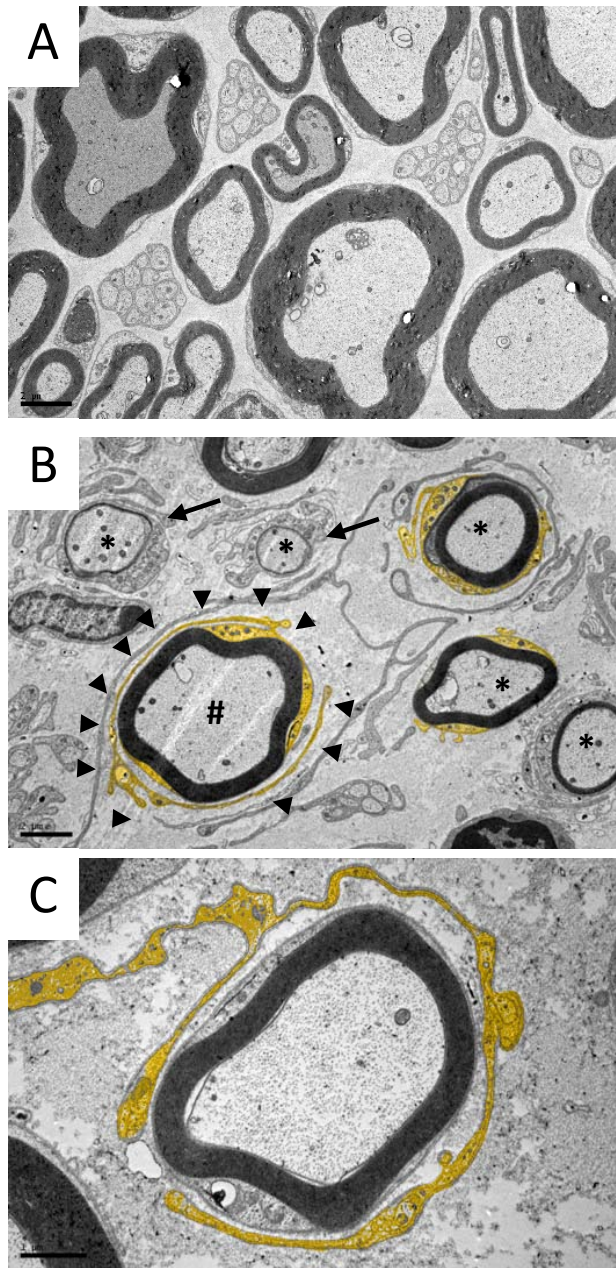
B



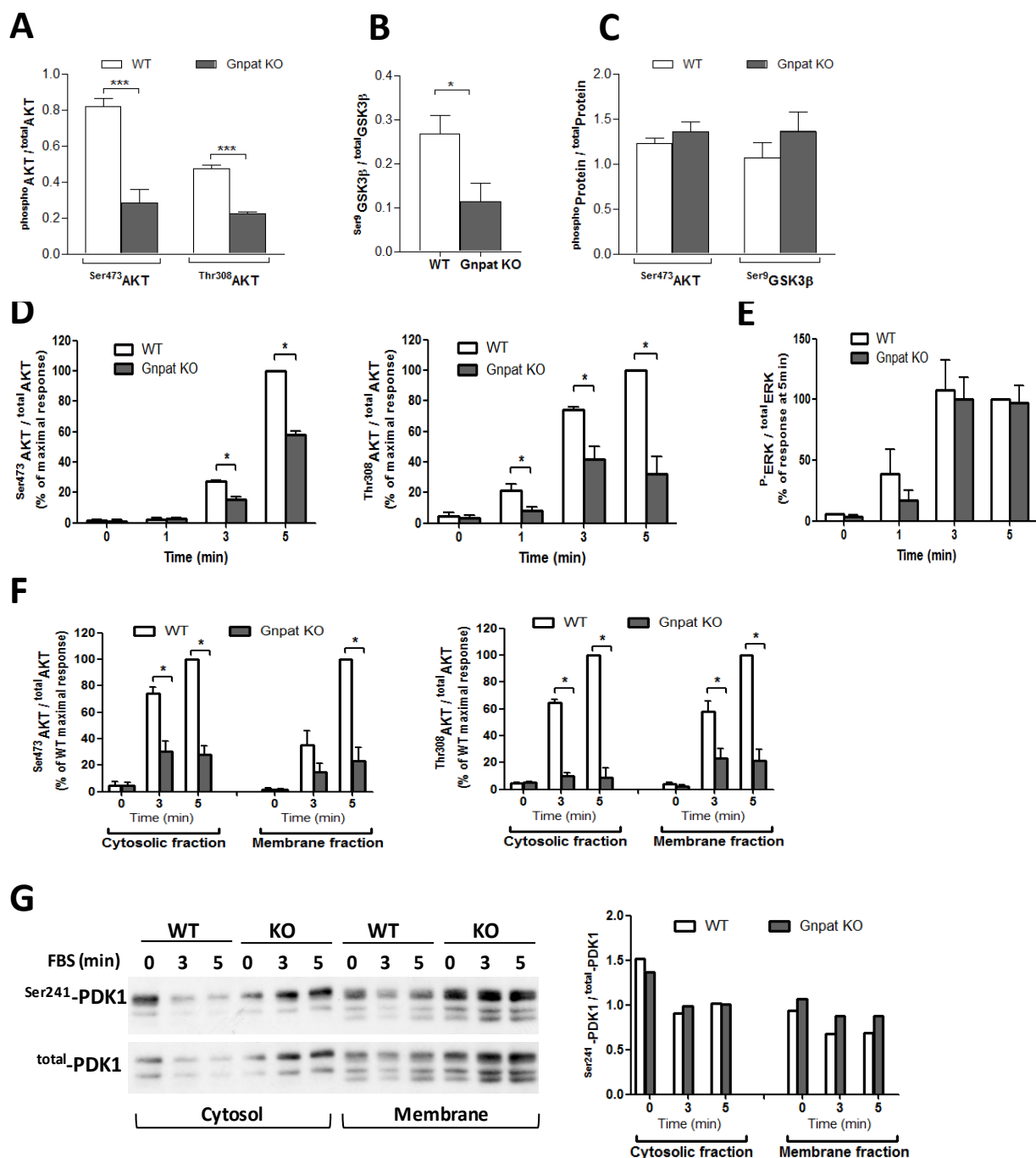
Supplementary Figure 1 – Impaired axonal sorting leads to the re-organization and myelination of Remak bundles from plasmalogen-deficient mice. Ultrastructural analysis of nerves from WT and *Gnpat* KO mice at P15 (**A**) and 17-months of age (**B**) revealed the presence of myelinated bundles of small and large (asterisks) caliber axons in mutant nerves. Scale bar is 2 μ m in **A**, and 1 μ m in **B**.



Supplementary Figure 2 –Histological assessment of sciatic nerves from WT, *Pex7* KO and *Gnpat* KO mice. (A) Sciatic nerves were isolated from 5, 10, 15 and 20 days old (P5, P10, P15, and P20, respectively) WT and plasmalogen-deficient mice, and stained with PPD to visualize myelin lipids. At all ages, nerves from *Pex7* and *Gnpat* KO mice showed thinner myelin sheaths. In nerves from *Pex7* and *Gnpat* KO at P5, the impairment in myelination can also be seen by the reduction in the number of myelinated fibers. Scale bar is 12μm. (B) Levels of myelin basic protein (MBP) in sciatic nerves from P10 and P90 WT and *Gnpat* KO mice.



Supplementary Figure 3– Ultrastructural analyses of sciatic nerves from aged WT and plasmalogen-deficient mice. Compared to WT nerves (**A**), sciatic nerves of 1.5 years old *Pex7* KO (**B**) and *Gnpat* KO mice (**C**) showed generalized axonal loss and demyelination was evident by the thinning of myelin sheaths (asterisks; (**B**)). Attempts of re-myelination were also detected (arrows in **B**). Schwann cells from plasmalogen-deficient mice extended multiple processes to enwrap demyelinated axons but surprisingly also myelinated axons (**C**). In mutant mice, we observed that myelinating Schwann cells could also extend processes (pseudocolored in yellow in **B** and **C**) in attempts to engulf itself (cardinal (#) and arrowheads in **B**) or other myelinating fibers (**C**). Scale bar in **A** and **B** is 2μm and in **C** is 1μm



Supplementary Figure 4—Plasmalogen deficiency specifically impairs AKT phosphorylation. (A) Quantification of phosphorylated AKT at Ser473 and Thr308 in sciatic nerves from WT and *Gnpat* KO at P4; *** $P < 0.003$. (B) Quantification of phosphorylated GSK3 β at Ser9 in sciatic nerves from WT and *Gnpat* KO at P4; * $P = 0.04$. (C) Quantification of phosphorylated AKT at Ser473 and GSK3 β at Ser9 in sciatic nerves from 3 months old WT and *Gnpat* KO. (D) Quantification of phosphorylated AKT at Ser473 and Thr308 in lysates from WT and *Gnpat* KO MEFs 0, 1, 3 and 5min after stimulation with 10% FBS. Mean values of three independent experiments. (E) Quantification of phosphorylated ERK1/2 in lysates from WT and *Gnpat* KO MEFs 0, 1, 3 and 5min after stimulation with 10% FBS. Mean values of three independent experiments; * $P < 0.01$. (F) Quantification of phosphorylated AKT at Ser473 and Thr308, in cytosolic and membrane fractions of MEFs from WT and *Gnpat* KO mice treated with 10% FBS for 0, 3 and 5 min. Mean values of three independent experiments. * $P < 0.01$. (G) Western blot analysis and quantification of PDK1 levels in cytosolic and membrane fractions of MEFs from WT and *Gnpat* KO mice revealed normal levels of active PDK1.